An assessment of contact metallization for high power and high temperature diamond Schottky devices

Sodjan Koné, Henri Schneider, Karine Isoird, Fabien Thion, Jocelyn Achard, Riadh Issaoui, Sabeur Msolli, Joël Alexis

An assessment of contact metallization for high power and high temperature diamond Schottky devices ☆

S. Koné [a,b], H. Schneider [a,b,*], K. Isoird [a,b], F. Thion [a,c], J. Achard [d], R. Issaoui [d], S. Msolli [e], J. Alexis [e]

[a] CNRS, LAAS, 7 avenue du Colonel Roche, F-31077 Toulouse, France
[b] Université de Toulouse, UPS, INSA, INP, ISAE, LAAS, F-31077 Toulouse, France
[c] CNRS, Laboratoire ampère, INSA-Lyon, 20, avenue Albert Einstein, F-69621 Villeurbanne, France
[d] CNRS, LSPM, Université Paris 13, 99 av. JB Clément, F-93430 Villetaneuse, France
[e] CNRS, LGP, ENI-TARBES, 47, avenue d'Azereix BP 1629, F-65016 Tarbes, France

Keywords:
Diamond
Power semiconductor devices
Schottky contact
Device characterization

A B S T R A C T

Different metals W, Al, Ni and Cr were evaluated as Schottky contacts on the same p-type lightly boron doped homoepitaxial diamond layer. The current–voltage (I–V) characteristics, the series resistance and the thermal stability are discussed in the range of RT to 625 K for all Schottky devices. High current densities close to 3.2 kA/cm^2 are displayed and as the series resistance decreases with increasing temperature, proving the potential of diamond for high power and high temperature devices. The thermal stability of metal/diamond interface investigated with regards to the Schottky barrier height (SBH) and ideality factor *n* fluctuations indicated that Ni and W are thermally stable in the range of RT to 625 K. Current–voltage measurements at reverse bias indicated a maximum breakdown voltage of 70 V corresponding to an electric field of 3.75 MV/cm. Finally, these electrical measurements have been completed with mechanical adhesion tests of contact metallizations on diamond by nano-scratching technique. These studies clearly reveal Ni as a promising contact metallization for high power, high temperature and good mechanical strength diamond Schottky barrier diode applications.

1. Introduction

Due to its exceptional properties, diamond is a very attractive material for power electronic switch devices. Its high electric breakdown field (E_c~10 MV/cm), high carriers mobilities (2200 cm^2/V.s for electrons [1] and 2200 cm^2/V.s for holes [2]) and low dielectric constant (ε_r~5.7) are suitable for high power and high frequency applications. In addition, the high bandgap (E_g~5.5 eV) and the unique thermal conductivity (20 W/cm.K) of diamond can be well exploited for a wide field of high temperature applications. Recent advances in synthesis of electronic grade single crystal intrinsic and boron doped diamond by chemical vapor deposition have unlocked the way to the development of diamond technologic processing for power electronic devices. This includes the steps of polishing, RIE etching, electrical contacts and edge termination structures. Among those steps, mastering electrical contacts on diamond is definitely a major issue. To date, ohmic contacts are obtained in a reproducible way on p-type boron doped diamond by depositing Ti/Pt/Au [3] and Si/Al [4] with low contact resistivity, around 10^{-6} Ω.cm^2, which is in agreement with electronic devices application requirements. However, studies on rectifier contacts in the literature face the difficulty to find suitable metals which form high Schottky barrier height, yield good mechanical adhesion and high thermally stable interface to diamond.

In this work, different metals W, Al, Ni and Cr were evaluated as Schottky contacts on the same lightly boron doped homoepitaxial diamond layer. The current–voltage (I–V) characteristics, the series resistance and the thermal stability are discussed in the range of RT to 625 K for all Schottky devices. Besides these electrical measurements, mechanical adhesion of contact metallizations on diamond is also investigated by nano-scratching technique.

2. Device test processing

p^+ and p^--type boron doped homoepitaxial diamond layers have been grown on 3×3 mm^2 HPHT Ib(100) diamond substrate. To prepare the substrate's surface prior to growth, a H_2/O_2 plasma etching pre-treatment has been performed [5]. Since the use of high microwave power densities strongly limits boron incorporation [6], medium microwave power (1500 W) and a pressure of 80 mbar have been used to deposit the 6 µm-thick heavily boron doped diamond layer (p^+) at a B/C ratio in the gas phase of 2000 ppm. The 1 µm-thick p^--layer was then deposited at a microwave power of 3000 W

☆ Presented at the Diamond 2011, 22nd European Conference on Diamond, Diamond-Like Materials, Carbon Nanotubes, and Nitrides, Budapest.

* Corresponding author at: CNRS, LAAS, 7 avenue du Colonel Roche, F-31077 Toulouse, France. Tel.: +33 5 61 33 69 96.
E-mail address: schneider@laas.fr (H. Schneider).

doi:10.1016/j.diamond.2012.05.007

and a pressure of 100 mbar and a B/C ratio reduced down to a few ppm. The resulting film was free of non-epitaxial crystals and SIMS measurements indicate a boron doping of $4 \cdot 10^{20}$ cm^{-3} and $3 \cdot 10^{17}$ cm^{-3} respectively in p^+ and p^--layers (Fig. 1).

By selective RIE etching, a 2×2 mm^2 p^--drift layer was insulated in the center of the substrate. Then, Ti/Pt/Au ohmic contact was deposed around the p^--layer on the etched out area (p^+-layer) and annealed at 500 °C under nitrogen flow for 1 h. Finally, circular Schottky contact metallizations W, Al, Ni, and Cr of 100 μm diameter were evaporated on the top of lightly B-doped layer by a same photolithography process (lift-off technique). Prior to each photolithography process, the p^--area sustained a chemical cleaning consisting in acetone, trichloroethylene and oxygen O_2 plasma treatment after water rinsing. Such cleaning process is effective to remove any organic contamination. Deposition of various Schottky metals on a same sample is very demanding technologically, but this solution provides the advantage to overcome reproducibility problems of diamond layers obtained by chemical vapor deposition (dislocations density, doping, thickness…). Thus, the characteristics obtained can be more easily correlated to metals. Fig. 2 shows the cross section and photography of the carried out structure with W (15 SBD devices), Al (12 SBD devices), Ni (12 SBD devices) and Cr (13 SBD devices) on the top of the p^- central area.

3. Results and discussion

3.1. Current–voltage characteristics from 300 K to 625 K

The current–voltage characteristics of Schottky devices were performed with an Agilent HP4142B analyzer from RT to 625 K. About half of the devices showed linear characteristics or excessively high reverse currents depending on their location on the p^--area mostly due to bulk defects (dislocations) which induce leakage paths in material [7,8] and near surface homogeneously distributed defects across the Schottky contact area which act electrically as highly doped and low barrier height regions [9]. Here we present the best results that were achieved for each type of contact metallization (Fig. 3).

Very high current densities in the range of 1600 A/cm^2–3200 A/cm^2 are found for Ni/diamond Schottky device at 5 V bias voltage in Fig. 3a. The changes in current–voltage (I–V) characteristics with temperature increase can be discussed in two separate phases depending on the competition between dopants activation process and thermal fall of carrier mobility. In the first step from RT to 525 K, the gradual thermal ionization of dopants outweighs the carrier mobility drop with temperature increase. Thus, the current density increases up to 3.2 kA/cm^2 at 525 K corresponding to the point of complete ionization of dopants.

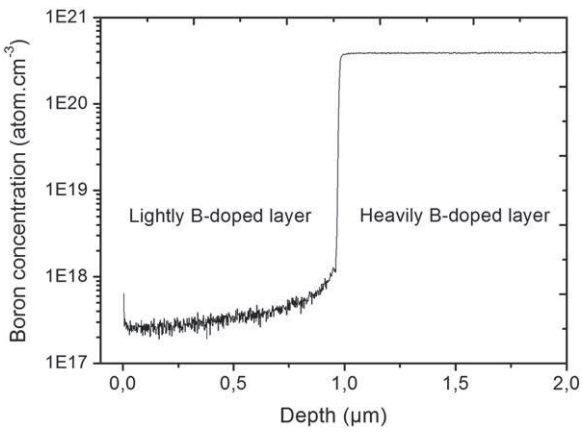

Fig. 1. SIMS profile in the lightly and the heavily B-doped diamond layers.

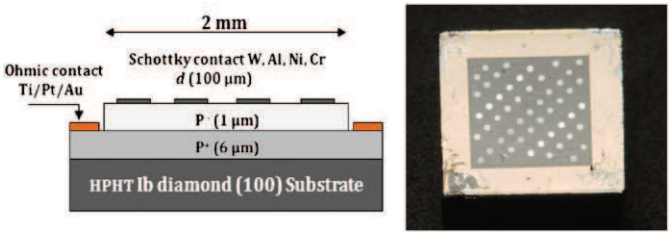

Fig. 2. Cross section and photography of the fabricated SBD device structure with W, Al, Ni, and Cr Schottky contacts on the top of the p^- central area.

In the second step (beyond 525 K), all dopants are ionized, the level of current output is then governed by the carrier mobility drop with temperature. Here, the current density goes down to 2.9 kA/cm^2 at 625 K. As far as the reverse operation is concerned, the Ni/diamond Schottky device shows very low reverse leakage current levels and no significant change can be noted in their thermal activation in the investigated temperature range.

For W/diamond Schottky device in Fig. 3b, an increase in current density from 550 A/cm^2 to 1000 A/cm^2 at 5 V bias voltage is revealed. In such contact metallization, a high resistivity to the current flow through most devices could be clearly observed compared to Ni/diamond devices. However, all of them yielded very low reverse leakage current levels as well as Ni contacts.

On Fig. 3c, high current densities from 600 A/cm^2 to 1300 A/cm^2 are highlighted at 5 V bias voltage in Al/diamond devices and very low reverse leakage currents are displayed up to 575 K where one can see the reverse current increases in $\times 3$ orders of magnitude. This behavior has been also observed in other Al devices. Such sudden degradation of reverse leakage current, due to a hard break of the Schottky barrier height, could be explained by the formation of a carbide layer at the Al/diamond interface. Indeed, Al is one of the well-known metals reacting easily with diamond at temperature and forming a carbide layer (aluminum carbide Al_4C_3). Few tens of nanometers of such layer are generally enough to change the carrier transport of Schottky barrier diodes [10].

As shown in Fig. 3d, the Cr/diamond device provides high current densities ranging from 1400 A/cm^2 to 3800 A/cm^2 at 525 K. But, these devices mostly displayed a chaotic evolution in (I–V) characteristics with an increase of temperature and high leakage current levels compared to other contact metallizations.

3.2. Devices series resistance as function of temperature

Another important property of a diode is its on-state series resistance $R_{on}S$ responsible for voltage drop across the device when forward biased. It should be as low as possible. Fig. 4 shows the electrical model of a Schottky barrier diode. The on-state voltage drop V_F across the device is the sum of the voltage drop due to the Schottky contact rectifying effect and voltage drops due to the low doped drift area (p^--layer) resistance R_D, the substrate (p^+-layer) resistance R_{sub} and the ohmic contact resistance R_C.

The on-state voltage drop V_F across the device is given by:

$$V_F = \frac{kT}{q} \cdot \ln\left(\frac{J_F}{J_S}\right) + (R_D + R_{sub} + R_C) \cdot J_F \quad (1)$$

where J_F and J_S are the forward current and the saturation current densities respectively.

The heavily doped p^+-layer is known as a very low resistive area. Moreover, the Au/Pt/Ti/diamond ohmic contact resistance is typically in the range of 10^{-6} Ω.cm^2.

Therefore, the on-state series resistance $R_{on}S$ across the device can be considered as mainly due the low doped drift area resistance R_D. It is measured here as a function of temperature from the dynamic

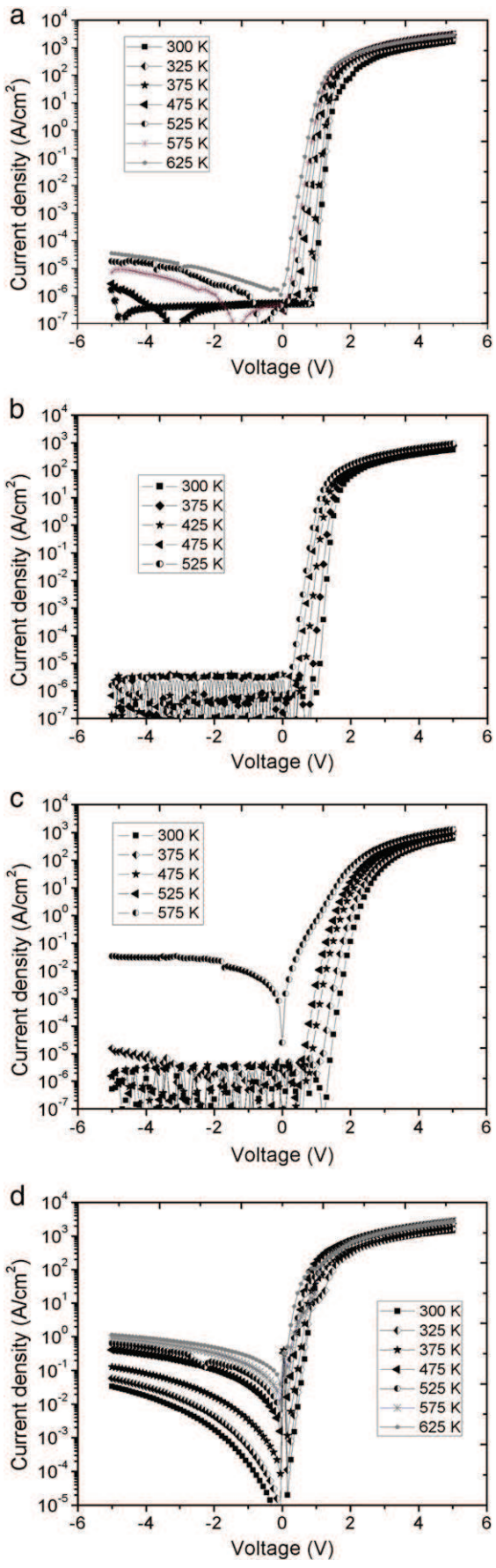

Fig. 3. Current–voltage (I–V) characteristics in the range of RT–625 K for Ni/diamond, W/diamond, Al/diamond and Cr/diamond SBD devices.

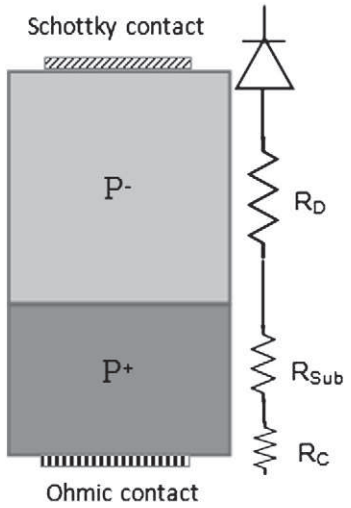

Fig. 4. Electrical modeling of Schottky barrier diode.

resistance extracted from the slope of (I–V) characteristics for each kind of Schottky metallizations. Fig. 5 shows each experimental data plotted as a function of temperature.

As one can note, the on-state resistance $R_{on}S$ decreases with an increase of temperature for all devices. Due to the deep boron acceptor level in diamond with an activation energy of 0.37 eV for boron concentrations well below the metal–insulator transition, only a small fraction of dopants is ionized at room temperature, making semiconductor diamond a poor electrical conductor at low temperature. The dopants ionization rate depending on the temperature, the more the temperature increases, the more the series resistance $R_{on}S$ decreases.

Otherwise, the series resistance differs depending on the Schottky metallization. This difference is probably related to the inhomogeneity of the active region (doping, dislocations, thickness…) and/or the difference in experimental SBH. It is therefore difficult to draw conclusions related to the type of metallization even when the nickel Ni device yields the lowest on-state series resistance $R_{on}S$ while the tungsten W is the most resistive.

3.3. Thermal stability of contacts metallizations on diamond

For high temperature applications, the thermal stability of metal/semiconductor interfaces is the main requirement for power electronic devices. The thermal stability has been investigated in the range of 300 K–625 K for each Schottky metallization regarding the Schottky barrier height (SBH) and the ideality factor (n) extracted from the current–voltage characteristics.

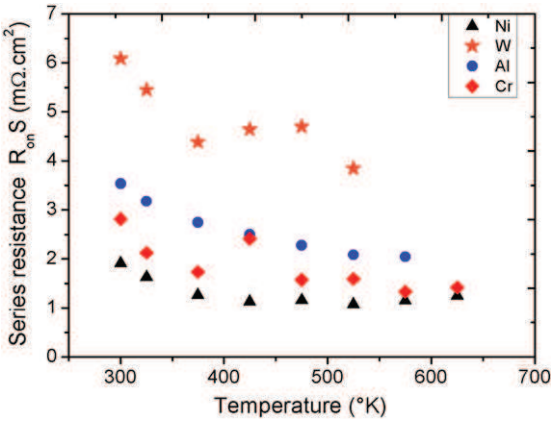

Fig. 5. On state series resistance $R_{on}S$ as temperature function.

The current transport mechanism in a Schottky barrier diode is governed by the thermionic emission (TE). The corresponding current–voltage (I–V) curve can be described by:

$$J = J_s\left[\exp\left(\frac{qV}{nkT}\right)-1\right]$$
$$J_s = A^*T^2S\exp\left(-\frac{q\Phi_B}{kT}\right) \quad (2)$$

where J_s is the saturation current density, n is the ideality factor, A^* is the Richardson constant (96 A/cm^2.K^2), $q\Phi_B$ is the Schottky barrier height (SBH) and S is the Schottky contact area.

For each temperature, the Schottky barrier height (SBH) was calculated from the saturation current density J_s determined by extrapolating the semilog forward (I–V) curve in the linear region at zero bias (V = 0) and the ideality factor (n) from the slope (a) of the expanded (I–V) curve according to Eqs. (3) and (4).

$$n = \frac{q}{kT}\cdot\frac{1}{a} \quad (3)$$

$$\Phi_B = \frac{kT}{q}\cdot\ln\left(\frac{A^*T^2}{J_S}\right) \quad (4)$$

Fig. 6 shows experimental data plotted as functions of temperature for each kind of Schottky metallization.

As the ideality factor is far above one ($n \gg 1$) in Al and Cr Schottky contacts, other carrier transport mechanisms interfere at the metal/diamond interface in addition to the thermionic emission. Indeed, tunneling and generation-recombination processes can occur through a Schottky contact in the case of extended defects and recombination centers in the space charge region respectively. These parasitic phenomena combine with interface traps density [11,12] are mainly responsible for barrier loss in Schottky rectifiers. Evidently in our case of study, a large gap occurs between the experimental and the theoretical SBH expected for Al and Cr contacts. The decrease of the ideality factor with increasing temperature is known as carrier transport process transition to thermionic emission exclusively, feature current transport mechanism in Schottky contacts [13].

In contrast, the ideality factor is extremely close to unity ($n \approx 1$) for W and Ni contacts and almost insensitive to temperature increase. This means that the current transport mechanism in these contacts is basically thermionic emission process. Moreover, the SBH stability indicates an insignificant chemical reactivity of W and Ni contacts to diamond. Thus, these contact metallizations can be considered as thermally stable in the range of 300 K–625 K.

3.4. Reverse bias voltage measurements

Current–voltage measurements at reverse bias have been performed immersing the sample in an insulating liquid (fluorine FC40). The insulating liquid avoids any electric field crowding at Schottky contact edges causing premature breakdown of the device. The results in Fig. 7 attest a maximum breakdown voltage V_{BR} near 50 V, 55 V and 70 V for Ni, Cr and Al contacts respectively. There is no correlation between the type of metallization and the SBD devices reverse operation limit given the uncertainty on the active layer homogeneity (thickness, doping and dislocations density).

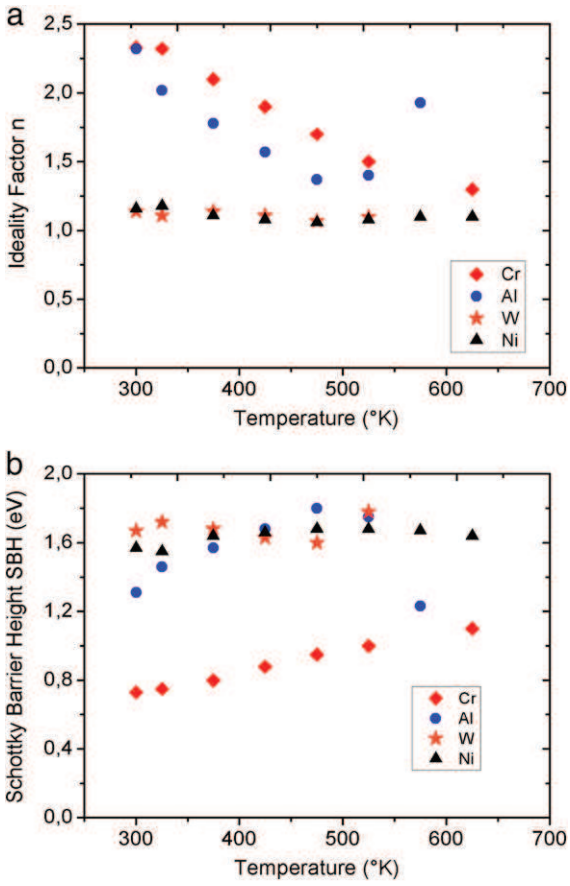

Fig. 6. The ideality factor (a) and the SBH (b) for W, Al, Cr and Ni Schottky contact to diamond as functions of temperature.

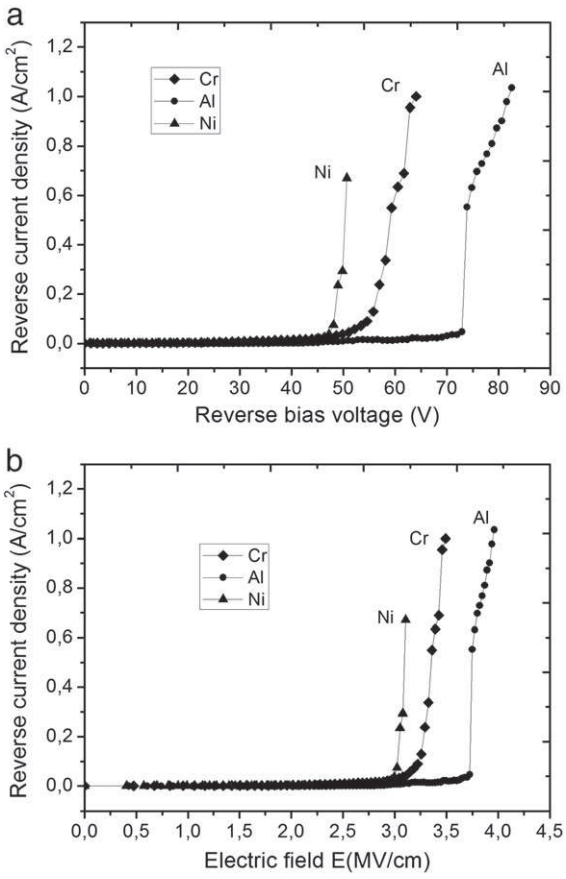

Fig. 7. Diamond SBD devices reverse operation limit as a function of: a) voltage, b) electric field.

Considering a triangular field distribution within the uniformly doped P^--layer, the breakdown voltage (V_{BR}) and the corresponding electric field (E_{max}) for unipolar power devices can be related by [14]:

$$V_{BR} \approx \frac{\varepsilon_s \cdot E_{max}^2}{2qN_A} \quad (5)$$

where ε_s is the dielectric constant (F/cm^{-2}), E_{max} is the maximum electric breakdown field (V/cm), q is the elementary charge (C), and N_A is the doping of p^--layer.

From Eq. (5), a maximum breakdown electric field of 3.75 MV/cm was calculated for the Al/diamond SBD device. This performance indicates that our diamond crystalline grade is in good agreement with the current state-of-the-art in CVD growth of single crystal diamond. Indeed, the growth of high quality single crystal CVD diamond meeting power electronic devices applications requirements still remains an important challenge. Consequently, practical performances of diamond based electronic devices are well below the theory. In the case of single crystal diamond SBDs in the literature, high reverse current levels are frequently observed and the maximum electric breakdown field does not exceed 4 MV/cm [15,16].

3.5. Schottky contacts adhesion on diamond

A good mechanical adhesion is also a major property for metal/semiconductor contacts. It is a key requirement for device bonding process and packaging technologies.

The Schottky contact metallizations studied above were deposited on a diamond sample by the same photolithography process previously described. Fig. 8 shows a photography of Cr, W, Ni and Al coatings on diamond sample.

The mechanical strength of metal coatings on diamond sample was investigated by nanoscratching technique at the Production Engineering Research Laboratory (LGP-Tarbes, France). Nanoscratching test is based on making scratches on the sample surface by moving a Berkovitch tip (indenter) in three successive steps and measuring their depth. This gives an opportunity to evaluate the hardness of coatings qualitatively.

- The first run of the indenter with a very low normal force applied (100 μN) determines the metal coating topography.
- The second run in which the applied force increases gradually until the maximum force imposed permits to evaluate the hardness of the metal coating.
- The third run in scratch background with the lowest applied force determines the metal coating spring back after scratching and the topography of the scratch sidewall.

The tests were carried out with a scratch speed of 10 μm/s, an imposed maximum force of 40 mN and a scratch distance of 200 μm. The indenter penetration curves as functions of scratch distance and the background from scratches are presented respectively in Fig. 9a and b for W, Al, Cr and Ni coatings.

Considering the scratch depths' importance in Fig. 9a, Al and W coatings seem to be less resilient to scratching. More specifically, tungsten contact behavior to scratching differs from other contact metallizations in Fig. 9b. Indeed, interfacial and structural disintegrations occur into the coating at low applied loads while no disintegration is observed in other coatings.

Furthermore, because of their low hardness, plastic deformations were observed in all coatings during the second run of the indenter as the normal force applied gradually increased.

However, the adhesion on diamond is stronger than the elasticity limit in the case of Ni, Cr and Al coatings. Also, scratch background inspections indicate that the mechanical dissipation in Cr and W coatings seems lower than in the Ni and Al coatings. In fact, cracks were observed on scratch sidewalls in the case of Cr and W coatings as shown in Fig. 9b.

These observations reveal that Ni and Al contacts exhibit good adhesion on diamond.

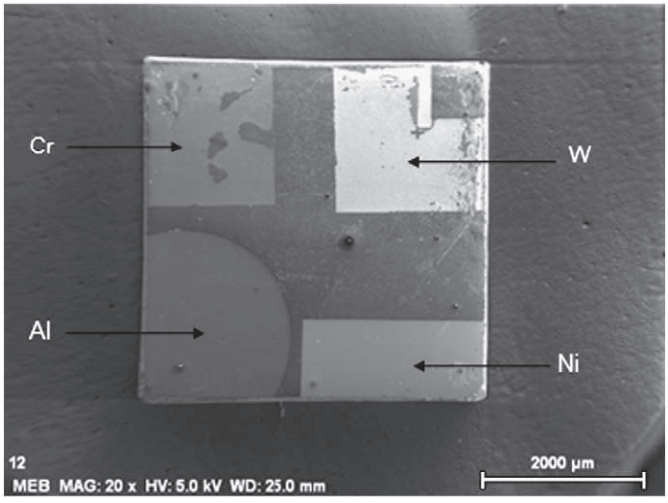

Fig. 8. SEM photography of Cr, W, Ni and Al coatings on diamond.

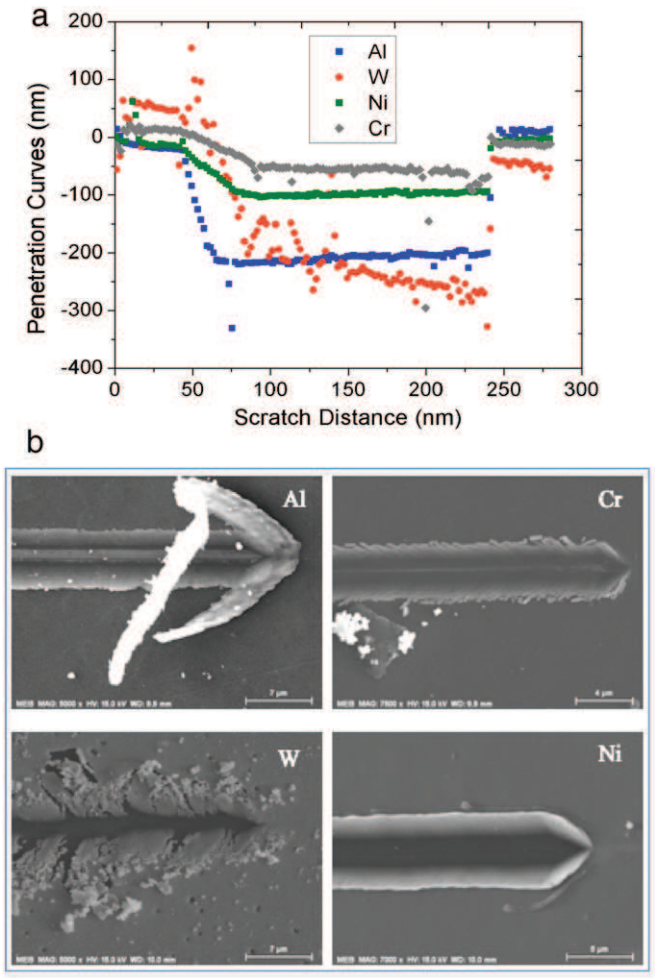

Fig. 9. a) Indenter penetration curves as functions of scratch distance, b) background from scratches.

Table 1
Experimental data related to Schottky contact metallization on diamond.

Contact metallization		W	Al	Cr	Ni
SBH (eV)	Φ_B	**1.67**	1.31	0.73	**1.57**
Threshold voltage (V)	V_{th}	**1.5**	2.5	**1**	1.7
Current density range (A/cm^2)	Forward J_F	550–1000	600–1300	**1400–2800**	**1600–3200**
	Reverse J_R	$\mathbf{10^{-7}}$–$\mathbf{10^{-5}}$	$\mathbf{10^{-7}}$–$\mathbf{10^{-5}}$	10^{-2}–1	$\mathbf{10^{-7}}$–$\mathbf{10^{-5}}$
Rectifying factor	J_F/J_R	10^9	10^9	10^5	$\mathbf{10^{10}}$
Series resistance ($m\Omega.cm^2$)	$R_{on}S$	6.1–3.85	3.54–2.04	2.81–1.33	**1.9–1.07**
Thermal stability	Qualitative analysis	Good	Good (≤300 °C)	Poor	Good
Adhesion	Qualitative analysis	Poor	Good	Fairly good	Good

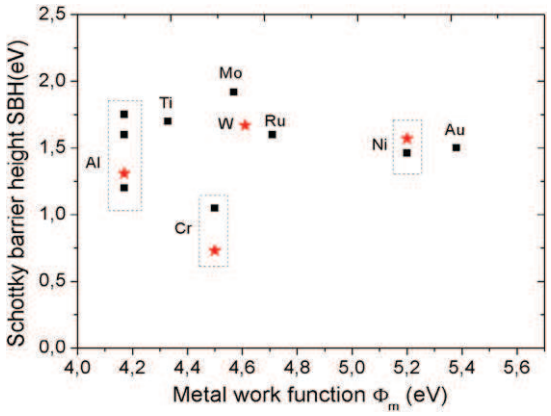

Fig. 10. The state of the art of SBH from various metal/diamond Schottky contacts, (■) = literature, (★) = this work.

4. Conclusion

Table 1 summarizes experimental data related to contact metallization evaluated in the range of RT–625 K. The best results for each criteria investigated are marked in bold.

Compared with the other contact metallizations, all of the experimental data in Table 1 indicate that nickel (Ni) is a suitable contact metallization for high power, high temperature and good mechanical strength diamond Schottky barrier diode applications.

In comparison to the state of the art of Schottky contacts on diamond, there is no work on mechanical adhesion and, moreover, the thermal stability is rarely investigated.

Thus, the only criteria for comparison that can be pointed here is the experimental Schottky barrier height (SBH).

Fig. 10 displays some experimental SBH data from various studies [7–22]. It is clear that our achievements are in good agreement with the state-of-the-art of Schottky contacts on diamond.

Acknowledgments

This work has been supported by the Aerospace Valley Cluster and the French National Research Agency ANR through project no. Blanc-06-2-134411. The authors acknowledge the collaborative effort of the CNRS-LAAS RTB clean room team.

References

[1] N. Tranchant, M. Nesladek, D. Thomson, Z. Remes, A. Bogdan, P. Bergonzo, Phys. Status Solid 204 (9) (2007) 2827–3200.
[2] T. Teraji, K. Arima, H. Wada, Toshimichi Ito, Appl. Phys. Lett. 96 (10) (2004) 5906–5908.
[3] Y. Chen, M. Ogura, S. Yamasaki, H. Okushi, Semicond. Sci. Technol. 20 (2005) 860–863.
[4] M. Werner, C. Johnston, P.R. Chalker, S. Romani, I.M. Buckley-Golder, J. Appl. Phys. 79 (1996) 2535.
[5] A. Tallaire, J. Achard, F. Silva, R.S. Sussmann, A. Gicquel, E. Rzepka, Phys. Status Solidi A 201 (2004) 2419.
[6] R. Issaoui, J. Achard, F. Silva, A. Tallaire, A. Tardieu, A. Gicquel, M.A. Pinault, F. Jomard, Appl. Phys. Lett. 97 (18) (2010) 3.
[7] R. Kumaresan, H. Umezawa, N. Tatsumi, K. Ikeda, S. Shikata, Diamond Relat. Mater. 18 (2–3) (February–March 2009) 299–302.
[8] Hitoshi Umezawa, Norio Tokuda, Masahiko Ogura, Sung-Gi Ri, Shin-ichi Shikata, Diamond Relat. Mater. 15 (11–12) (November–December 2006) 1949–1953.
[9] A. Vescan, W. Ebert, T. Borst, E. Kohn, Diamond Relat. Mater. 4 (1995) 661–665.
[10] M. Wade, P. Muret, F. Omnès, A. Deneuville, Diamond Relat. Mater. 15 (2006) 614.
[11] J. Tersoff, W.A. Harrison, Phys. Rev. Lett. 58 (1987) 2367.
[12] W. Mönch, Europhys. Lett. 27 (1994) 479.
[13] Tokuyuki Teraji, Yasuo Koide, Toshimichi Ito, Phys. Status Solidi RRL 3 (2009) 211.
[14] L.M. Tolbert, B. Ozpineci, S.K. Islam, M.S. Chinthavali, Power Energy Syst., Proc., 2003, pp. 317–321.
[15] A. Vescan, I. Dauville, P. Gluche, W. Ebert, E. Kohn, Diamond Relat. Mater. 7 (1998) 581–584.
[16] D.J. Twitchen, A.J. Whitehead, S.E. Coe, J. Isberg, J. Hammersberg, T. Wikström, E. Johansson, IEEE Trans. Electron. Devices 51 (5) (May 2004) 826–828.
[17] J. Butler, M.W. Geis, K.E. Krohn, J. Lawless, S. Deneault, Semicond. Sci. Technol. 18 (2003) S67–S71.
[18] Y.G. Chen, M. Ogura, H. Okushi, N. Kobayashi, Diamond Relat. Mater. 12 (2003) 1340–1345.
[19] M. Craciun, Ch. Saby, P. Muret, A. Deneuville, Diamond Relat. Mater. 13 (2) (2004).
[20] K. Ikeda, H. Umezawa, K. Ramanujam, S. Shikata, Appl. Phys. Expr. 2 (2009) 011202.
[21] D. Takeuchi, S. Yamanaka, H. Okushia, Diamond Relat. Mater. 11 (2002) 355–358.
[22] H. Umezawa, S. Shikata, 21st International Symposium on Power Semiconductor Devices & IC's, ISPSD, 14–18 June 2009, IEEE, 2009, p. 259.